

Published in final edited form as:

Hippocampus. 2012 June ; 22(6): 1242–1255. doi:10.1002/hipo.20998.

Selective presynaptic terminal remodeling induced by spatial, but not cued, learning: a quantitative confocal study

R. McGonigal¹, N. Tabatadze¹, and A. Routtenberg^{1,2,3}

¹Department of Psychology, Northwestern University, Evanston, IL

²Department of Neurobiology, Northwestern University, Evanston, IL

³Department of Physiology, Feinberg School of Medicine, Northwestern University, Chicago, IL

Abstract

The hippocampal mossy fibers (MFs) are capable of behaviorally-selective, use-dependent structural remodeling. Indeed, we previously observed a new layer of Timm's staining induced in the *stratum oriens* (SO) in CA3 after spatial but not cued water maze learning (Rekart et al., *Learn. Mem.* 2007; 14:416–421). This led to the prediction that there is a learning-specific induction of presynaptic terminal plasticity of MF axons. The present study confirms this prediction demonstrating, at the confocal level of analysis, terminal-specific and behavior-selective presynaptic structural plasticity linked to long-term memory.

Male adult Wistar rats were trained for 5d to locate a hidden or visible platform in a water maze and a retention test was performed 7d later. MF terminal subtypes, specifically identified by an antibody to zinc transporter 3 (ZnT3), were counted from confocal z-stacks in the *stratum lucidum* (SL) and the SO. In hidden platform trained rats there was a significant increase in the number of large MF terminals (LMTs, 2.5–10 μ m diameter, >2 μ m² area) compared to controls both in the proximal SL ($p < 0.05$) and in the SO ($p < 0.01$). Surprisingly, there was no detectable increase in small MF terminals (SMTs, 0.5–2 μ m diameter, <2 μ m² area) in either SL or SO as a consequence of training. This distinction of the two MF terminal types is functionally important as LMTs synapse on CA3 pyramidal neurons, while SMTs are known to target inhibitory interneurons.

The present findings highlight the pivotal role in memory of presynaptic structural plasticity. Because the 'sprouting' observed is specific to the LMT, with no detectable change in the number of the SMT, learning may enhance net excitatory input to CA3 pyramidal neurons. Given the sparse coding of the MF-CA3 connection, and the role that granule cells play in pattern separation, the remodeling observed here may be expected to have a major impact on the long-term integration of spatial context into memory.

Keywords

Hippocampus; mossy fibers; ZnT3; memory; plasticity

Introduction

Neural plasticity after learning involves a coordinated structural change in both presynaptic and postsynaptic morphology. There is abundant evidence for learning-dependent postsynaptic dendritic spine plasticity in which an increase in number of spines, structural

remodeling or enhanced motility has been described (Moser et al., 1994; Engert and Bonhoeffer 1999; Matus 2000; Segal and Andersen 2000; Alvarez and Sabatini 2007; Harvey and Svoboda 2007; Holtmaat and Svoboda 2009; Xu et al., 2009, Yang et al., 2009). However, there is a relative paucity of information on the role of presynaptic plasticity.

As discussed by Chklovskii et al (2004), it is known that axons have the capacity for growth after development, largely based on studies reporting axonal remodeling induced by lesions and injury (Darian-Smith and Gilbert 1994; Florence et al., 1998; Yamahachi et al., 2009). However, such axonal plasticity is the result of pathological mechanisms and thus does not reflect the intrinsic ability of the axon to change in response to experience in the adult. Although LTP-induced sprouting does not speak directly to the issue of whether axonal growth can be induced specifically by learning and memory, there are a few reports of axonal sprouting of mossy fibers in the hippocampus associated with LTP induction (e.g., Adams et al., 1997; Escobar et al., 1997).

In vertebrates, observations of presynaptic structural plasticity associated with learning have been limited. In the invertebrate *Aplysia* a role for presynaptic structural plasticity in learning and memory was demonstrated by: an increase in the number of active zones and the number of vesicles per active zone; the persistence in the number of axon varicosities at the time of testing memory retention (Bailey and Chen, 1983, 1989). In studies that primarily focus on postsynaptic changes in vertebrates, incidental observations of changes to presynaptic boutons were also noted (e.g., West and Greenough, 1972). In the mouse, environmental enrichment (EE) causes an increase in the number of hippocampal mossy fiber (MF) terminals and presynaptic active zones (Gogolla et al., 2009), while memory precision in the water maze correlates to an increase in the number of filopodia per core MF terminal (Ruediger et al., 2011). Moreover, the retraction and expansion of axons and filopodia have been observed under basal conditions both *in vivo* and in organotypic slice culture (De Paola et al., 2003, 2006; Tashiro et al., 2003; Galimberti et al., 2006; Stettler et al., 2006; Nishiyama et al., 2008; Yamahachi et al., 2008), which suggest that adult axons do indeed have the capacity to undergo structural change associated with normal physiological functions.

A potential role for presynaptic structural plasticity in long-lasting memory has been observed in the mossy fiber system (for review see Rekart et al., 2007b). The MFs, axons arising from dentate gyrus granule cells (GCs), are part of the classical trisynaptic circuit and can be highly dynamic in nature (Henze et al., 2000; De Paola et al., 2003; Galimberti et al., 2006; Gogolla et al., 2009). Our work is inspired by the original observations of Adams et al. (1997) and Escobar et al. (1997) that showed LTP can induce MF growth, and Ramirez-Amaya et al. (2001) that reported a dramatic learning-induced increase in Timm's staining within the hippocampal SO. In our previous studies, the MF growth only occurred after learning the location of a hidden platform; but no such MF redistribution was observed after training to locate a visible platform (Rekart et al., 2007a; see Routtenberg, 2010, for review). Corresponding immunostaining with the axonal marker Tau1, zinc transporter 3 (ZnT3) that is specifically localized to MF bouton synaptic vesicle membranes (Palmiter et al., 1996; Wenzel et al., 1997), and the presynaptic vesicle marker synaptophysin, has strengthened the hypothesis that the MF growth represents an increased number of presynaptic MF terminals that are induced by spatial learning (Holahan et al., 2006).

To test this hypothesis directly the present study quantified learning-induced presynaptic terminal remodeling as visualized at the confocal level. Because MFs possess two discrete and specialized types of presynaptic terminals with distinct cellular targets (Acsády et al., 1998; Henze et al., 2000) we determined whether learning would differentially influence remodeling of either terminal type. Finally, we evaluated the laminar distribution of both

terminal types to determine whether a re-organization of terminals might occur in the absence of a change in absolute terminal number. Such a readjustment would then suggest the participation of a homeostatic process.

Materials and Methods

Subjects

50 day old male Wistar rats (WR; n=26) were purchased from Charles River and housed in groups of 3 with free access to food and water. The temperature (22°C) and lighting (lights on from 0600 to 1800 hrs) of the animal housing unit were controlled. Animal care conformed to guidelines of the National Institute of Health Guide for the Care and Use of Laboratory Animals and guidelines set by the Northwestern University Animal Care and Usage Committee.

Water maze training procedure

All training was performed in a circular pool (110cm in diameter) located in a room lit by three inverted lights with extramaze cues on each of the surrounding walls. The pool was filled with water kept at 22 (+ 2)°C, and made opaque by black nontoxic tempera paint. Rats were separated into 4 groups and run as Hidden (n=9), Visible (n=4), Yoked swim control (n=4) and Not trained (n=9). Prior to training rats were handled for 4 min/day for 4 days. The hidden platform group was trained to find a platform submerged 1cm below the water surface using extramaze cues only, while the visible platform group were trained to find a platform with a cue attached positioned above the water surface. Yoked swim controls spent the same amount of time in the water as the hidden group but no escape platform was present. A black curtain surrounded the pool during training of the visible platform and yoked controls to prevent exposure to extramaze cues. Not trained rats were handled only and received no water maze training. It was important to control for the potential effects of activity in this study as it has been suggested that exercise can promote growth of MFs into the SO (Toscano-Silva et al., 2010). However the latter study involved extended periods of intensive exercise such as running in a wheel and previous reports from our laboratory have shown no significant MF growth in swim control groups. Water maze training consisted of 8 trials/ day for 5 days. For each trial animals were given 60s to locate the platform from which they were removed after 30s once found. Rats were guided to the platform if they did not locate the platform within 60s. A 60s retention or 'probe' test in which the platform was removed was performed 7 days later and the time spent in each quadrant and the number of platform crossings was recorded using the HVS Image system (HVS) and analyzed using the public domain Wintrack system (D. Wolfer; <http://www.dpwolfer.ch/wintrack/Index.htm>).

Tissue processing and Immunohistochemistry

After the retention test, rats designated for the confocal studies (n=4/group) were immediately euthanized by a rising concentration of CO₂; brains were then removed, hemisected and processed for Timm's and immunofluorescent staining. Five hidden platform trained rats and 5 not trained rats were part of a separate study using viral-mediated axonal tracing to be described below. The hemisphere for Timm's staining was immersed in 1% Na₂S for 16 min prior to fixation overnight in a solution of 3% gluteraldehyde/4% paraformaldehyde in 0.1M phosphate buffered saline (PBS) at 4°C. The other hemisphere was fixed overnight in 4% paraformaldehyde/ 0.1M PBS also at 4°C. Immersion solutions were changed the following day to 30% sucrose/0.1M PBS before cryosectioning at 30µm in the coronal plane. Sections were collected into 0.1% sodium azide/0.1M PBS. Every fifth section in the septal hippocampus between Bregma -2.30 to -3.14mm was selected from each hemisphere for analysis. The rationale for this selection range is based on a previous report that demonstrated training-induced growth of mossy fibers into the SO of the septal

hippocampus that is not observed within the temporal pole (Ramirez-Amaya et al., 2001). Thus we chose to focus our study on the analysis of the most anterior hippocampus within the region of the most prominent MF field expansion. Sections were mounted, incubated in Timm's stain (50% Gum Arabic, 5% hydroquinone, 5% citric acid, 1% silver nitrate) for 90min at 32°C in complete darkness before counterstaining with cresyl violet. Three sections per animal were selected for immunofluorescent staining. Sections were washed 3 times in 0.1M tris-buffered saline (TBS) + 0.5% Triton X-100 (T-TBS), blocked for 1h at R.T. in 3% NGS + T-TBS (blocking solution) before staining overnight at 4°C in primary antibody in blocking solution. Primary antibodies were used with the following titers: 1:250 rabbit anti- ZnT3 (kind gift of Dr. R. Palmiter); 1:500 mouse anti-synaptophysin (Sigma); 1:500 mouse anti-NeuN (Chemicon). Sections were washed 3 times in T-TBS before incubation for 2h in secondary antibody in blocking solution. Alexa488-conjugated goat anti-rabbit or Alexa594-conjugated goat anti-mouse secondary antibodies from Invitrogen/Molecular probes (Carlsbad, CA) were used at a 1:500 dilution. To ensure specificity of immunolabeling, primary antibodies were omitted in control tissue. Immunofluorescently labeled sections were mounted onto slides and covered with Vectashield Hardset mounting medium with DAPI nuclear counterstain (Vector Labs) and coverslipped. To facilitate direct comparison of measurements in both SO and SL across treatment groups, all tissue processing was carried out in parallel.

Imaging and Quantification

To assess MF remodeling, the area of Timm's staining in the SO was compared to the SL in three anterior hippocampal sections from each rat. This was measured by a grid-counting method, as previously described (Holahan et al., 2006). Briefly, images of the entire CA3 were captured using a 10× objective on an Olympus BX61 microscope with a DP70 camera (12.5 megapixels). A grid (squares= 25µm/side) was placed over the entire hippocampus. The number of points of the grid overlaying Timm's staining in either the SL or SO from the tips of the granule cell blades to the CA3/CA2 border were multiplied by the area of each box to estimate the area of staining in each lamina. From these data the SO:SL ratio was calculated. To measure SL width, a line from the mid-point between the suprapyramidal blade of the dentate gyrus and the pyramidal cell layer between the two granule cell blades was drawn that followed the trajectory of the pyramidal cell layer past the tips of the blades (procedure illustrated in Figure 1C *right*). Using this line as a guide, the width of the SL from the SL/SR border, to the SL/SP border was measured. Differences in cutting angle among brains could conceivably contribute to a variation in width measurements made within the hippocampus. Specifically, this could be due to a subtle variation in tilt in the plane of section away from the frontal plane. However, it seems likely that the effects reported would be robust as such variability will only result in an underestimation and therefore only compromise the magnitude of the changes detected.

The number of ZnT3 identified LMTs across the entire width of the SL were quantified from adjacent confocal z-stacks from each of 3 sections per rat captured using a Zeiss 510 Meta System with a 60× water-immersion objective. MF terminals consist of two populations (Figure 8A): **large MF terminals (LMT)**, 2.5–10µm in diameter (as designated by Acsády et al., 1998) that predominantly synapse on thorny excrescences located in the proximal 100µm of the CA3 pyramidal cell apical dendrites. Each MF gives rise to 10–18 LMTs that are arranged *en passant* or attached by a side branch as a satellite LMT to a parent core LMT; **small MF terminals (SMT)** are 0.5–2µm in diameter and predominantly target local inhibitory interneurons (Acsády et al., 1998). As shown schematically in Figure 8A, SMTs are also arranged in two configurations: at the end of filopodial extensions projecting from LMT, or as *en passant* boutons. ZnT3 positive LMT and SMT were defined 3-dimensionally by analysis of z-stacks consisting of 0.8µm thick z-slices taken at an interval of 0.4µm.

Terminals were identified in this study by double-labeling ZnT3-positive terminals with the presynaptic terminal marker synaptophysin. Additionally, to demonstrate the distinction between SMTs and LMTs, we have used viral (herpes simplex virus, HSV) mediated delivery of GFP to granule cells, to fill the terminal arbor and thus measure the area range of MF terminals (Figure 4). The areas of such terminals were measured using a known scale after using the tracing tool in ImageJ software to outline each labeled terminal. As shown in Figure 4D, the terminal areas did not follow a normal distribution but instead a bimodal distribution, which we designate as SMTs and LMTs. These profiles strengthen the basis for our designation of similar sized profiles of ZnT3 and synaptophysin stained presynaptic terminals seen on the confocal microscope (Figure 5A and B). LMTs were defined as having profiles of ZnT3 staining more than $2.5\mu\text{m}$ in their longest axis and more than $2\mu\text{m}^2$ in area, irregular in shape and present in at least seven z-slices taken at an interval of $0.4\mu\text{m}$, while SMTs were defined as having profiles less than $2\mu\text{m}$ in diameter, $0.5\text{--}2\mu\text{m}^2$ in area and present in no more than 5 z-slices taken at an interval of $0.4\mu\text{m}$. NeuN staining was used to label pyramidal neurons to identify the SP border that separates the SL and the SO on either side of the SP. A grid (squares = $10\mu\text{m}/\text{side}$, $100\mu\text{m}^2$ ROI) overlaying each z-stack was used to count LMT number at $10\mu\text{m}$ intervals across the SL at three different dorsal-ventral positions. LMTs overlaying the right and upper grid-square borders were included in the count, while LMTs spanning the left and lower border were excluded. The number of LMTs per $100\mu\text{m}^2$ ROI across the SL were plotted every $10\mu\text{m}$ for each group and repeated measures ANOVA used to calculate statistical significance. Total number of terminals in the SL per group was also calculated and one-way ANOVA used to test for statistical significance. To quantify MF puncta in the proximal SL ($0\text{--}80\mu\text{m}$ from SP border), and in the SO, a confocal z-stack ($90\times 90\times 10\mu\text{m}$) from each of 3 sections per rat were first captured using a Zeiss 510 Meta System with a $100\times$ oil immersion objective through both the SL and SO. LMT and SMT number in three $100\mu\text{m}^2$ ROI at four set positions ($10\text{--}20$, $30\text{--}40$, $50\text{--}60$, $70\text{--}80\mu\text{m}$) across the breadth of the SL from the NeuN identified SP border were initially counted and compared between groups. Statistical significance was determined by repeated-measures ANOVA for distance versus group, and one-way ANOVA for puncta number at the most proximal SL position ($10\text{--}20\mu\text{m}$ from the SP border) versus group. Four $100\mu\text{m}^2$ ROI in the SO at a set distance of $30\mu\text{m}$ from the SP/SO border identified by NeuN staining were used to quantify SMT and LMT number. One-way ANOVA was used to test statistical significance among groups. All quantification was performed using ImageJ software (NIH) under blind conditions.

HSV-GFP injections

In hidden platform trained rats ($n=5$) and not trained control rats ($n=5$) herpes simplex virus (HSV)-mediated delivery of green fluorescent protein (GFP; generous gift of Dr Rachael Neve; expression of fluorescent protein is driven by the cytomegalovirus (CMV) promoter) was used to further study the distribution of each MF terminal subtype, and specifically whether training increases the MF terminal area distribution. Unlike the marker ZnT3 which selectively labels synaptic vesicles within the MF terminals, the GFP can be expressed in all cells, including granule cells and their MF axons and terminals. Its advantage is that it labels the terminal *in its entirety*, which enables the area of each terminal type to be easily quantified. Rats were anaesthetized under inhalant isoflurane and placed in a stereotaxic frame before the cranial surface was exposed. A 26 gauge Hamilton syringe was used to unilaterally infuse $2\mu\text{l}$ of HSV-GFP ($1\mu\text{l}$ medially, $1\mu\text{l}$ laterally) into the DG granule cell layers to primarily label MFs (AP: -3.2mm ; ML: -1 and -2mm ; DV: -5 and -4.5mm) at a rate of $0.1\mu\text{l}/\text{min}$. Injections were carried out 2 days before the probe test was run. Preliminary results showed this to be the optimal interval between delivery and good quality GFP expression within MFs. After probe test, brains were immersion fixed in 4% paraformaldehyde/ 0.1M PBS at 4°C and the following day placed in 30% sucrose/ 0.1M

PBS before cryosectioning at 30 μ m in the coronal plane. Every fifth section between Bregma -2.30 to -3.14 mm was selected and mounted for presynaptic terminal analysis and probe placement. Confocal z-stacks (90 \times 90 \times 10 μ m) were captured across the SL to the SO from each of 3 sections per rat using a 100 \times oil immersion objective. In these studies we identified and quantified the size distinction of the two MF terminals labeled with GFP. The area of 40 individual presynaptic terminal profiles was measured from each section using the selection tool in ImageJ after a set threshold had been applied to the image. The number of terminals per area range was plotted for both trained and not trained animals and an analysis of normal distribution per group performed (Shapiro-Wilk test). We found a bimodal distribution of areas which we designated as SMT (0.5–2 μ m²) and LMT (>2 μ m²) (Figure 4B and C). Core LMT were identified as those positioned along a MF axon and more than 2 μ m² in area, while satellite LMT, also more than 2 μ m² in area, were attached by a filopodial extension to core LMT. All quantification was performed using ImageJ software (NIH) under blind conditions.

Statistical analysis

Statistical tests used: One-way ANOVA; repeated-measures ANOVA was used to measure latency and number of terminals across the SL; Shapiro-Wilk test was used to test for a normal distribution of terminal area and a Student *t*-test was used to test the difference in area of terminals in HSV-GFP injected animals compared to control. Significance was set at $p < 0.05$.

Results

1. Learning-induced ‘thinning’ of MF terminal field in SL

a. Acquisition and retention—During acquisition, the latency to reach the platform was initially lower for rats trained to locate the visible platform versus those trained to find the hidden platform (Figure 1A, repeated-measures ANOVA $F(1,11)=7.2$, $p<0.05$). The latency was similar between the training groups by the completion of training, as shown in Figure 1A. Although hidden and visible platform trained rats exhibit equivalent performance on the water maze at the end of 5 days of training, only the hidden platform trained group form a spatial memory of the platform location as revealed in a retention test 7 days later. This ‘probe test’ revealed that rats trained to find a hidden platform spent significantly more time in the region where the platform had been (annulus) than visible platform trained or yoked swim control rats (One-way ANOVA $F(2, 16)=7.68$, $p<0.01$, Fig 1B).

b. MF redistribution in SL: ‘Laminar thinning’—Closer inspection of the Timm’s staining distribution uncovered a previously unreported finding: the width of MF terminal field innervation in the SL in hidden platform trained animals was reduced in thickness (Figure 1C and indicated by red arrows in Figure 1D). This ‘laminar thinning’ of the SL MF innervation was statistically significant both by a group effect (One-way ANOVA $F(3,12)=5.89$, $p<0.05$) as well as by a post-hoc analysis which showed that the hidden platform group had a significantly reduced SL width compared to all other training groups ($p<0.05$, Fisher’s LSD tests). The width of staining across the SL did not significantly differ between the visible platform trained, yoked swim control and not trained groups. These new findings could be compromised by not taking into account plane of sectioning variations. But because such variations would likely increase variability, it may be that the statistical significance of the current thinning measurement is actually an underestimation of the differences. Because this thinning directly relates to the concomitant thickening seen in SO and the compression of LMTs in SL (see Figure 6), one sees the coordination of these 3 event as converging on a plasticity scenario in which dynamic readjustments of MFs both in SL and in SO are part of an integrated remodeling program set into motion by spatial

memory formation. A similar reduction in SL width was observed when staining for the MF specific marker ZnT3 (Figure 1E). Additionally staining for ZnT3 and the presynaptic terminal marker protein synaptophysin were both found in the SL for all training groups (Figure 2). With these two markers one observed 'laminar thinning' only in the SL of hidden platform trained animals. The width of staining in the SL did not fall below 100 μ m for any group, suggesting that there may be a preserved minimal proximal length of dendrite that maintains MF innervation.

2. MF terminal field remodeling: translaminar growth into SO

The hidden, but not the visible, platform trained rats demonstrate an increased area of Timm's staining in the SO (Figure 3A), as described previously (Rekart et al., 2007a). This area is significantly larger when compared to all other groups as determined by calculating the SO:SL ratio in Timm's stained tissue (Fig 3B, one-way ANOVA $F(3,12)=5.44$, $p<0.05$; post hoc Hidden vs. Visible $p<0.01$; Hidden vs. Yoked swim control $p<0.01$; Hidden vs. not trained $p<0.05$). Using the MF specific marker ZnT3 an increase in staining area is observed in the SO; as with Timm's stain this is only detectable in hidden platform trained animals as compared to the other training groups (Figure 3A). There is also a parallel increase in synaptophysin staining in the SO (Figure 2); the staining pattern for all of these markers strongly supports the conclusion that the new layer of staining consists of MF terminals.

3. Selective remodeling of large, but not small, presynaptic MF terminals within SL

To first characterize the MF terminal types, we labeled terminals (see Material & Methods) by HSV-GFP delivered to dentate gyrus GCs so as to fill MF terminals with GFP, enabling a computation of terminal area and then size distribution (Figure 4). We found that there was a non-normal distribution of terminal areas (Shapiro-Wilk test, $p<0.05$) which was best characterized as bimodal. One mode was designated as containing SMTs, which were less than 2 μ m² in area, while the LMT were more than 2 μ m² in area (Figure 4D). Figure 4C shows that the LMTs positive for HSV-GFP can be co-labeled with ZnT3 antibody indicating that counted GFP labeled terminals are of MF origin. This is important as HSV-GFP labels GCs predominantly, but not exclusively. Therefore, this is a sampling from the MF population but would appear to represent a good approximation of MFs in the total population. The ZnT3 co-labeling and the bimodal distribution support such a conclusion. Moreover, while we will show changes in laminar distribution and terminal number as a consequence of training, the size distribution remained unaffected (Figure 4D). The nearly identical bimodal distribution observed in 2 separate analyses of different hippocampal tissue, in not trained and trained animals, points to the reliability of the quantitative method implemented. Importantly, because the training itself does not alter the presynaptic terminal size distribution, it suggests that these 2 terminal types maintain a size constancy in the face of structural rearrangements of LMTs.

The existence of two clearly differentiated presynaptic terminal types raises the question of their differential participation in learning-induced presynaptic remodeling. To address this issue we assessed MF terminal remodeling at the confocal level by counting small and large MF puncta 7 days after the 5 day training period. Having established the criteria that distinguish the two terminal types, we then stained the entire population of MF terminals with ZnT3 antibody and separately counted LMTs and SMTs based on these morphological features (as described in Materials and Methods). Examples of ZnT3 and synaptophysin identified LMT and SMT that were subsequently counted are illustrated in Figures 5A and 5B.

We first directed our attention to the SL region where we found an increase in LMT number adjacent to the SP border in hidden platform trained rats (Figure 6A). Further from SP, but

still in the SL, there was a rapid decline in LMT number which approached a zero value at a distance of 150 μm from SP. This decrement could thus account for the thinning described previously (Figure 1C). The number of LMT in the other 3 groups also declined, but more gradually, with distance which extended up to 200 μm from the SP border. We found there was, indeed, a significant interaction between distance and group (repeated-measures ANOVA, $F(14,53)=2.84$, $p<0.01$, Figure 6A) suggesting that the LMT number in each group changed differentially with distance from the CA3 cells as described. An important observation was that the total number of LMT between groups remained the same (one-way ANOVA $F(3,12)=1.53$, $p=0.26$, Figure 6B). To examine this change in intra-laminar distribution of LMT in more detail in the 0–80 μm region of SL, we analyzed confocal z-stacks captured at 100 \times magnification at four positions (10–20, 30–40, 50–60 and 70–80 μm , Figure 6C) from the SL/SP border. Figure 6C (*left*) demonstrates that there was a significant effect of distance ($F(3,36)=7.04$, $p<0.01$, repeated-measures ANOVA) and group ($F(3,12)=14.49$, $p<0.001$) on LMT number per 100 μm^2 from 10 to 80 μm . Further analysis showed that the number of LMTs per 100 μm^2 was significantly greater at the closest position (10–20 μm) to the SP/SL border in hidden platform trained rats compared to all other groups (Hidden vs. Visible $p<0.05$; Hidden vs. Yoked swim control $p<0.01$; Hidden vs. not trained $p<0.001$; Fig 6D, *left*). We have designated this apparently unique redistribution of terminals from the outer to the inner SL as ‘homeostatic compression’ because of the increase in density of innervation in the proximal CA3 apical dendrite region and the lack of change in total number of LMT in the SL lamina.

We were surprised to find that in this same SL region we could not detect any change in either number or distribution of SMTs among groups. This in contrast to changes in distribution or LMT number counted within the proximal SL. Similar to LMTs, the number of SMTs decreased with distance from the SP border (repeated-measures ANOVA $F(3,36)=7.24$, $p<0.01$, Figure 6C, *right*) but the number of SMTs across the proximal region of SL was not significantly different among groups (repeated-measures ANOVA $F(3,12)=0.89$, $p=0.475$, Figure 6C, *right*). At the closest position to the SL-SP border, there was also no significant training-induced difference in SMT ($p=0.169$, Figure 6D, *right*). Therefore, within the SL, and in contrast to LMTs, spatial learning induced no detectable change in density or distribution of SMTs per μm^2 relative to controls.

4. Specific remodeling of large, but not small, presynaptic MF terminals within SO

Would a change in a particular MF terminal population in SO be responsible for the previously reported learning-induced increase in SO staining? We found that ZnT3 positive LMT number per 100 μm^2 did increase in the SO with hidden platform training; while there was no significant difference in LMT number among the visible platform trained, yoked swim control and not trained groups. (One-way ANOVA $F(3,12)= 8.4$, $p<0.01$; post-hoc Hidden vs. Visible $p<0.01$; Hidden vs. Yoked swim control $p<0.05$; Hidden vs. not trained $p<0.001$; Fig 7A). In contrast to LMTs, but paralleling the results seen in the SL, there was no significant change to SMT number in the SO among the 4 groups (One-way ANOVA $F(3,12)=0.24$, $p=0.86$, Figure 7B).

Discussion

In the present study the entire MF terminal population was stained with the MF terminal specific ZnT3 antibody (Palmiter et al., 1996; Wenzel et al., 1997). Two distinct MF terminal subtypes, SMT and LMT, were identified and quantified at the confocal level by both ZnT3 immunohistochemistry and viral-mediated GFP labeling of MFs. We then studied the effects of water maze training and memory formation on number and distribution of these two MF terminal populations.

Learning-induced structural plasticity selective for large presynaptic MF terminals (LMTs)

On the basis of the present confocal study demonstrating a selective increase in LMT, we conclude that our earlier observations of learning-induced MF remodeling (see Introduction) may be directly related to an increase in LMT number within the SO. In contrast, we did not detect any change in SMT number or distribution after learning. To our knowledge this is the first report of a learning-selective (hidden but not visible platform training) and presynaptic terminal-specific (LMT but not SMT) structural change in the rat hippocampus.

While we cannot rule out a minor contribution of newly-born GC axons to the expansion of the MF field, this mechanism seems unlikely to underlie the remodeling reported here given the fact that it takes 10 days for new-born granule cell axons to grow into the CA3 (Zhao et al., 2006) and we see robust growth into SO only 7 days after training in Wistar rat, and synaptogenesis only 2 days later in the Long Evans rat (Holahan et al., 2006). Therefore we have instead attributed this expansion to new innervation related to MF sprouting into the SO and compression within the SL (see Figure 8).

Specificity of MF terminal identification and remodeling

At the same time that the present report was submitted, Ruediger et al. (2011), described results that appear to differ from our own findings. They detected a learning-induced elevation in the number of filopodial SMTs that emanate from a core LMT in mice. These SMTs synapse on inhibitory interneurons in the CA3 and contribute to feed-forward inhibition in this region. Elevations were seen after both contextual fear-conditioning and water maze training. It was also reported by Ruediger et al. (2011) that there was a more modest, yet still significant, increase in the number of putative synapses, identified as bassoon positive puncta, within GFP labeled core LMT, after fear conditioning, but no change in overall LMT density.

Why did these authors not observe a learning-induced change in overall LMT number similar to that reported here? We think that their findings and conclusions likely contrast with the results of this study largely due to their MF sampling strategies. First, MF terminals were detected in Thy1-GFP transgenic mice, which express GFP in less than 20% of the total MF population (Vuksic et al., 2008). Therefore, it is possible that there was not an adequate sampling from the MF terminal population. This sampling contrasts with the present study where all MF terminals were specifically labeled and thus available for analysis. Second, as reported by Galimberti et al (2010) even though the same construct is used, their transgenic mice have different patterns of GC and MF labeling depending on the Thy1-GFP line chosen. Importantly the transgenic mouse line used by Ruediger et al. (Thy1-GFP *Ls1*) exhibits only 30–35% labeled MFs that possess one terminal arborization (TA), which is described by Galimberti and colleagues as the site of plasticity. The rest of the MF terminals along the same labeled axon apparently do not undergo remodeling. Moreover, all of the other GFP labeled MFs express no TAs and thus would not be expected to express LMT plasticity. By using this particular mouse line, Ruediger et al. may have limited the opportunity to observe learning-induced LMT plasticity. The population sampling thus calls into question the representative nature of the labeled terminals studied and may explain the lack of increase in LMT as an index of change within the whole MF population.

Ruediger et al. (2011) report a change in filopodia number which is consistent with the evidence that axonal filopodia are known to be highly dynamic and plastic in response to activity (De Paola et al., 2003; Tashiro et al., 2003; Nishiyama et al., 2008). The method employed to investigate presynaptic plasticity of filopodia in these transgenic mice involved quantifying the average number of filopodia per LMT. Given the LMT sampling issues mentioned above, however, quantification of these SMTs might not be representative of the

population. In addition, the quantitative approach used does not take into consideration any simultaneous changes potentially occurring in the *en passant* SMT population. As the overall number of SMTs has indeed been shown to be stable (De Paola et al., 2003), it is possible that there is no change in absolute SMT number in the transgenic mice after learning. This intrinsic stability in the SMT population could also explain why in the current study we do not detect a change to SMT number as we sample from the whole population. Moreover, all filopodia were included in the analysis by Ruediger et al (2011) regardless of whether the filopodia possessed bassoon positive varicosities at their ends or not. Additionally, it is unclear whether contact with interneuron dendrites was identified for each case. This suggests that although an increase in filopodia number may have been detected in response to learning, a proportion of the filopodia counted would probably not make synapses and thus would not contribute to feed-forward inhibition. In our studies we only identified those terminals possessing synaptic vesicle proteins (ZnT3 and synaptophysin), which makes it more likely that the terminals counted were putative synapses.

Another critical point to consider is the rather dramatic difference between the plasticity of MFs in rat and mouse (Rekart et al., 2007c). Using Timm's stain of *mouse hippocampus* to identify MF terminal field innervation, there was no detectable learning-induced MF remodeling in SL or SO, even when the paradigm was modified to achieve asymptotic learning performance. Therefore it is perhaps not surprising that there exists a discrepancy in the nature of MF terminal remodeling described in rats in the present study to that seen in mice by Ruediger et al. (2011). Despite the sampling issues in the Ruediger et al. report, and the species differences just considered, both studies call attention to learning-induced presynaptic remodeling of mossy fibers as a potentially critical mechanism of plasticity underlying the memory formation process.

What is the physiological consequence of MF terminal remodeling?

Evidence that MF transmission is, in fact, responsible for long-lasting memory comes from studies that show that the blockade of MF – CA3 transmission interferes with spatial learning and memory (LaSalle et al., 2000; Holahan and Routtenberg, 2011). The mechanism interfered with is not known but perhaps it is caused by disruption of spatial pattern separation processes (Kesner, 2007). Evidence to suggest that MF structural remodeling is directly associated with memory storage is provided by studies reporting memory-impairment and attenuation of MF growth by blockade of activity during water maze training with NMDA receptor antagonist MK801 (Ramirez-Amaya et al., 2001) or lidocaine (Holahan and Routtenberg, 2011).

It has been proposed that even subtle adjustments in structural plasticity could have a major impact on networks with sparse connections (Chklovskii et al., 2004) such as those found between MFs and the CA3 (McNaughton and Morris, 1987, Amaral et al., 1990). Due to the sparse coding and powerful 'detonating' MF-CA3 synapse, it is expected that an increase in MFCA3 transmission would enhance pattern separation processes important for spatial information storage in this network (Treves and Rolls, 1992, 1994).

The physiological consequence of spatial learning-induced MF terminal compression in the SL and sprouting in the SO (see Figure 8) would likely result in a net increase in CA3 throughput. Recordings from CA3 principal cells after DG stimulation *in vitro* (Kobayashi and Poo, 2004) and with conditioned learning *in vivo* (Segal and Olds, 1972; Thompson et al., 1996) demonstrate an increase in excitability of these neurons. Additionally, MF sprouting into the inner molecular layer in the dentate gyrus of kainate-treated epileptic rats results in an increased post-synaptic depolarization of granule cells suggesting that the new recurrent MF terminals excite granule cells (Otsu et al., 2000). These studies give additional credibility to our suggestion that increased MF sprouting enhances MF-CA3 transmission

thereby increasing the efficiency of pattern separation processing leading to long-term information storage.

The learning-induced structural plasticity reported here not only encompasses the addition of new LMTs into the SO, but also the homeostatic rearrangement of LMT within the SL. There are other examples of such homeostatic regulation of terminal number that support the possibility that circuit output can be altered by a rearrangement of terminals rather than a change to the total number. Cheetham et al (2008) have reported on the relocation of portions of axons in the sensory cortex during reorganization after whisker trimming to a “region of closer proximity” with dendritic spines. This enhances the capacity for new synapses to be formed rapidly after whisker deprivation and likely accounts for the strengthening of excitatory unitary connections observed in spared cortex that is not accounted for by alterations in dendritic spine density (Cheetham et al., 2007). Barnes and Finnerty (2010) suggested that relocating synapses to different dendritic branches of the same cell could be a strategy used to change the output networks without changing the number of synapses. Moreover, Bourne and Harris (2011) describe a reduction in both excitatory and inhibitory synapse number that coordinates with an increase in synapse size during LTP leading to a net stability of the number of post-synaptic elements in the CA1 after the induction of theta-burst stimulation in hippocampal slices. These examples of post-synaptic structural homeostasis complement our findings of apparent presynaptic structural homeostasis in SL as learning induces an increase in terminal number in proximal SL along with a decrease in distal SL so that the absolute terminal number remains unchanged.

Activity-dependent MF structural plasticity

The present evidence suggests that activity-dependent remodeling set into motion by spatial learning and memory formation is selective for LMTs. Consistent with these observations previous studies have revealed that neuronal activity regulates LMT size and complexity in hippocampal slice cultures (Galimberti et al., 2006). It may have been expected that an increase in LMTs would require a simultaneous increase in SMTs to dampen potentially pathologically high levels of CA3 pyramidal cell excitation (Lawrence and McBain, 2003; McBain 2008). The lack of a detectable change in number or distribution of SMTs may be relevant to a prior report which noted that with network activation, the total number of this population is quite stable over time (De Paola et al., 2003). Moreover, while SMT input is initially depressed with GC and LMT activation (Maccafferri et al., 1998), a study by Pelkey et al. (2005) demonstrated that SMT activity can in fact be re-established after LTD, therefore it is likely that a certain amount of inhibitory terminal homeostatic regulation will always be in place.

Hippocampal Mechanisms of Memory: Persistence of structural changes

It has been suggested in the Standard Model of Memory Consolidation that the hippocampus does not have a long-term function in memory so that neurons can be recycled for new memories (e.g., Alvarez and Squire, 1994). In the present study long-term memory was defined by the 7 day period after the completion of training but the coordinated structural change may persist for at least 30 days (Holahan et al., 2006; Ramirez-Amaya et al., 2001; Rekart et al., 2007a). Interruption of CA3 transmission at the conclusion of each daily training session in the water maze task by injection of lidocaine had little effect on 5-day acquisition (Holahan and Routtenberg, 2011). However, 7 days after the last lidocaine injection there was a significant reduction in translaminal MF growth along with an impairment in memory for the target quadrant compared to vehicle injected controls. In a study by Kleim et al (2004), significant motor cortex re-mapping and cortical synaptogenesis were observed after 7–10 days, but not 3 days, of motor skill learning. As reorganization in the motor cortex only occurred after 7 days of training it was suggested

that this level of remodeling is required for consolidation rather than acquisition. So too in the present study where the MF remodeling may represent a key substrate change that is necessary for storage of this long-term spatial memory, at least for 30 days (Ramirez-Amaya et al., 2001). The present results are thus consistent with the multiple trace hypothesis of Moscovitch et al. (2006).

Are post-synaptic changes coordinated with presynaptic terminal remodeling?

Though our report focuses on the link between presynaptic terminal growth and long-term memory, the existence of a coordinated postsynaptic growth process cannot be doubted. A major focus of learning-induced structural plasticity has indeed been placed on the outgrowth and motility of dendritic filopodia (Moser et al., 1994; Engert and Bonhoeffer, 1999; Matus 2000; Segal and Andersen 2000; Alvarez and Sabatini 2007; Xu et al., 2009, Yang et al., 2009). Colicos et al (2001) have shown that there is an activity-dependent, coordinated remodeling *in vitro* of both pre- and postsynaptic structures; new postsynaptic structures are associated with functional presynaptic structures and could therefore mediate enhanced synaptic transmission.

This view may apply to synaptic growth in hippocampus after spatial learning. LMTs typically synapse on specialized pyramidal dendritic spines, termed thorny excrescences (TE). It will be of interest to determine whether there is a coordinated induction of TEs along with the increased LMTs observed after learning. Considering that MF contact with CA3 cell dendrites precedes post-synaptic TE formation during development (Amaral and Dent, 1981; Gaiarsa et al., 1992), and that kainate-induced MF sprouting can then lead to ectopic TE formation on GCs (Represa et al., 1993), it is tempting to predict that similar TE induction will occur after learning-induced MF sprouting.

A proposed MF remodeling scenario: compression and sprouting

The suggested presynaptic terminal learning-induced remodeling events discussed above can be schematically summarized in a simplified diagram (Figure 8) which calls attention to two probable processes of plasticity that may be occurring after learning. In one scenario, *Sprouting*, there is a proliferation of growth, emanating from existing axonal arbors, that then populates the SO. This is consistent with our finding of an increase in the number of LMTs in SO. In the other scenario, *Compression*, there is an apparent learning-induced shift of existing LMT terminals from the outer SL to the inner SL, giving rise to the significant elevation of LMTs in proximal SL. It is attractive to think that these ongoing structural plasticity processes are the substrate for the hippocampal-neocortical indexing function of pattern separation that is then stored within this circuitry (Teyler and Rudy, 2007).

Acknowledgments

This work was supported by research grant NIMH MH54326-07 to A.R. The authors are grateful to Drs. R. Palmiter and R. Neve for generously providing the ZnT3 antibody and HSV-GFP, respectively. We would also like to thank Mr Brian Lin for his excellent technical help in the behavioral training of the rodents.

Grant sponsor: NIMH; Grant Number: MH54326-07

References

- Acsády L, Kamondi A, Sik A, Freund T, Buzsáki G. GABAergic cells are the major postsynaptic targets of mossy fibers in the rat hippocampus. *J Neurosci.* 1998; 18(9):3386–3403. [PubMed: 9547246]
- Adams B, Lee M, Fahnestock M, Racine RJ. Long-term potentiation trains induce mossy fiber sprouting. *Brain Res.* 1997; 775(1–2):193–197. [PubMed: 9439843]

- Alvarez P, Squire LR. Memory consolidation and the medial temporal lobe: a simple network model. *Proc Natl Acad Sci USA*. 1994; 91(15):7041–7045. [PubMed: 8041742]
- Alvarez VA, Sabatini BL. Anatomical and physiological plasticity of dendritic spines. *Ann Rev Neurosci*. 2007; 30:79–97. [PubMed: 17280523]
- Amaral DG, Dent JA. Development of the mossy fibers of the dentate gyrus: I. A light and electron microscopic study of the mossy fibers and their expansions. *J Comp Neurol*. 1981; 195(1):51–86. [PubMed: 7204652]
- Amaral DG, Witter MP. The three-dimensional organization of the hippocampal formation: a review of anatomical data. *Neuroscience*. 1990; 31(3):571–591. [PubMed: 2687721]
- Bailey CH, Chen M. Morphological basis of long-term habituation and sensitization in *Aplysia*. *Science*. 1983; 220(4592):91–93. [PubMed: 6828885]
- Bailey CH, Chen M. Structural plasticity at identified synapses during long-term memory in *Aplysia*. *J Neurobiol*. 1989; 20(5):356–372. [PubMed: 2664078]
- Barnes SJ, Finnerty GT. Sensory experience and cortical rewiring. *Neuroscientist*. 2010; 16(2):186–198. [PubMed: 19801372]
- Bourne JN, Harris KM. Coordination of size and number of excitatory and inhibitory synapses results in a balanced structural plasticity along mature hippocampal CA1 dendrites during LTP. *Hippocampus*. 2011; 21(4):354–373. [PubMed: 20101601]
- Cheetham CE, Hammond MS, Edwards CE, Finnerty GT. Sensory experience alters cortical connectivity and synaptic function site specifically. *J Neurosci*. 2007; 27(13):3456–3465. [PubMed: 17392462]
- Cheetham CE, Hammond MS, McFarlane R, Finnerty GT. Altered sensory experience induces targeted rewiring of local excitatory connections in mature neocortex. *J Neurosci*. 2008; 28(37):9249–9260. [PubMed: 18784305]
- Chklovskii DB, Mel BW, Svoboda K. Cortical rewiring and information storage. *Nature*. 2004; 431(7010):782–788. [PubMed: 15483599]
- Colicos MA, Collins BE, Sailor MJ, Goda Y. Remodeling of synaptic actin induced by photoconductive stimulation. *Cell*. 2001; 107(5):605–616. [PubMed: 11733060]
- Darian-Smith C, Gilbert CD. Axonal sprouting accompanies functional reorganization in adult cat striate cortex. *Nature*. 1994; 368(6473):737–740. [PubMed: 8152484]
- De Paola V, Arber S, Caroni P. AMPA receptors regulate dynamic equilibrium of presynaptic terminals in mature hippocampal networks. *Nat Neurosci*. 2003; 6(5):491–500. [PubMed: 12692557]
- De Paola V, Holtmaat A, Knott G, Song S, Wilbrecht L, Caroni P, Svoboda K. Cell type-specific structural plasticity of axonal branches and boutons in the adult neocortex. *Neuron*. 2006; 49(6):861–875. [PubMed: 16543134]
- Engert F, Bonhoeffer T. Dendritic spine changes associated with hippocampal long-term synaptic plasticity. *Nature*. 1999; 399(6731):66–70. [PubMed: 10331391]
- Escobar ML, Barea-Rodríguez EJ, Derrick BE, Reyes JA, Martínez JL Jr. Opioid receptor modulation of mossy fiber synaptogenesis: independence from long-term potentiation. *Brain Res*. 1997; 751(2):330–335. [PubMed: 9099823]
- Florence SL, Taub HB, Kaas JH. Large-scale sprouting of cortical connections after peripheral injury in adult macaque monkeys. *Science*. 1998; 282(5391):1117–1121. [PubMed: 9804549]
- Galimberti I, Gogolla N, Alberi S, Santos AF, Müller D, Caroni P. Long-term rearrangements of hippocampal mossy fiber terminal connectivity in the adult regulated by experience. *Neuron*. 2006; 50(5):749–763. [PubMed: 16731513]
- Galimberti I, Bednarek E, Donato F, Caroni P. EphA4 signaling in juveniles establishes topographic specificity of structural plasticity in the hippocampus. *Neuron*. 2010; 65(5):627–642. [PubMed: 20223199]
- Gaiarsa JL, Beaudoin M, Ben-Ari Y. Effect of neonatal degranulation on the morphological development of rat CA3 pyramidal neurons: inductive role of mossy fibers on the formation of thorny excrescences. *J Comp Neurol*. 1992; 321(4):612–625. [PubMed: 1380521]

- Gogolla N, Galimberti I, Deguchi Y, Caroni P. Wnt signaling mediates experience-related regulation of synapse numbers and mossy fiber connectivities in the adult hippocampus. *Neuron*. 2009; 62(4):510–525. [PubMed: 19477153]
- Harvey CD, Svoboda K. Locally dynamic synaptic learning rules in pyramidal neuron dendrites. *Nature*. 2007; 450(7173):1195–1200. [PubMed: 18097401]
- Henze DA, Urban NN, Barrionuevo G. The multifarious hippocampal mossy fiber pathway: a review. *Neuroscience*. 2000; 98(3):407–427. [PubMed: 10869836]
- Holahan MR, Rekart JL, Sandoval J, Routtenberg A. Spatial learning induces presynaptic structural remodeling in the hippocampal mossy fiber system of two rat strains. *Hippocampus*. 2006; 16(6): 560–570. [PubMed: 16685708]
- Holahan MR, Routtenberg A. Lidocaine injections targeting CA3 hippocampus impair long-term spatial memory and prevent learning-induced mossy fiber remodeling. *Hippocampus*. 2011; 21(5): 532–540. [PubMed: 20865723]
- Holtmaat A, Svoboda K. Experience-dependent structural synaptic plasticity in the mammalian brain. *Nat Rev Neurosci*. 2009; 10:647–658. [PubMed: 19693029]
- Kesner RP. Behavioral functions of the CA3 subregion of the hippocampus. *Learning & Memory*. 2007; 14:771–781. [PubMed: 18007020]
- Kleim JA, Hogg TM, VandenBerg PM, Cooper NR, Bruneau R, Remple M. Cortical synaptogenesis and motor map reorganization occur during late, but not early, phase of motor skill learning. *J Neurosci*. 2004; 24(3):628–633. [PubMed: 14736848]
- Kobayashi K, Poo MM. Spike train timing-dependent associative modification of hippocampal CA3 recurrent synapses by mossy fibers. *Neuron*. 2004; 41(3):445–454. [PubMed: 14766182]
- Lawrence JJ, McBain CJ. Interneuron diversity series: containing the detonation--feedforward inhibition in the CA3 hippocampus. *Trends Neurosci*. 2003; 26(11):631–640. [PubMed: 14585604]
- Lassalle JM, Bataille T, Halley H. Reversible inactivation of the hippocampal mossy fiber synapses in mice impairs spatial learning, but neither consolidation nor memory retrieval, in the Morris navigation task. *Neurobiol Learn Mem*. 2000; 73(3):243–257. [PubMed: 10775494]
- Maccaferri G, Toth K, McBain CJ. Target-specific expression of presynaptic mossy fiber plasticity. *Science*. 1998; 279(5355):1368–1370. [PubMed: 9478900]
- Matus A. Actin-based plasticity in dendritic spines. *Science*. 2000; 290(5492):754–758. [PubMed: 11052932]
- McBain CJ. Differential mechanisms of transmission and plasticity at mossy fiber synapses. *Prog Brain Res*. 2008; 169:225–240. [PubMed: 18394477]
- McNaughton BL, Morris RGM. Hippocampal synaptic enhancement and information storage within a distributed memory system. *Trends Neurosci*. 1987; 10:408–415.
- Moser MB, Trommald M, Andersen P. An increase in dendritic spine density on hippocampal CA1 pyramidal cells following spatial learning in adult rats suggests the formation of new synapses. *Proc Natl Acad Sci USA*. 1994; 91(26):12673–12675. [PubMed: 7809099]
- Moscovitch M, Nadel L, Winocur G, Gilboa A, Rosenbaum RS. The cognitive neuroscience of remote episodic, semantic and spatial memory. *Curr Opin Neurobiol*. 2006; 16(2):179–190. [PubMed: 16564688]
- Nishiyama H, Fukaya M, Watanabe M, Linden DJ. Axonal motility and its modulation by activity are branch-type specific in the intact adult cerebellum. *Neuron*. 2008; 56(3):472–487. [PubMed: 17988631]
- Otsu Y, Maru E, Ohata H, Takashima I, Kajiwara R, Iijima T. Optical recording study of granule cell activities in the hippocampal dentate gyrus of kainate-treated rats. *J Neurophysiol*. 2000; 83(4): 2421–2430. [PubMed: 10758143]
- Palmiter RD, Cole TB, Quaife CJ, Findley SD. ZnT-3, a putative transporter of zinc into synaptic vesicles. *Proc Natl Acad Sci USA*. 1996; 93(25):14934–14939. PMID: PMC26240. [PubMed: 8962159]
- Pelkey KA, Lavezzari G, Racca C, Roche KW, McBain CJ. mGluR7 is a metaplastic switch controlling bidirectional plasticity of feedforward inhibition. *Neuron*. 2005; 46(1):89–102. [PubMed: 15820696]

- Ramirez-Amaya V, Escobar ML, Chao V, Bermúdez-Rattoni F. Synaptogenesis of mossy fibers induced by spatial water maze overtraining. *Hippocampus*. 1999; 9(6):631–636. [PubMed: 10641755]
- Ramirez-Amaya V, Balderas I, Sandoval J, Escobar ML, Bermúdez-Rattoni F. Spatial long-term memory is related to mossy fiber synaptogenesis. *J. Neurosci*. 2001; 21(18):7340–7358. [PubMed: 11549744]
- Rekart JL, Sandoval CJ, Bermudez-Rattoni F, Routtenberg A. Remodeling of hippocampal mossy fibers is selectively induced seven days after the acquisition of a spatial but not a cued reference memory task. *Learn Mem*. 2007a; 14(6):416–421. [PubMed: 17554086]
- Rekart, J.L.; Holahan, M.R.; Routtenberg, A. Presynaptic Structural Plasticity and Long-Lasting Memory: Focus on Learning-Induced Redistribution of Hippocampal Mossy Fibers. Chapter 5. In: Bermúdez-Rattoni, F., editor. *Neural Plasticity and Memory: From Genes to Brain Imaging*. Boca Raton (FL): CRC Press; 2007b. 2007
- Rekart JL, Sandoval CJ, Routtenberg A. Learning-induced axonal remodeling: evolutionary divergence and conservation of two components of the mossy fiber system within Rodentia. *Neurobiol Learn Mem*. 2007c; 87(2):225–235. [PubMed: 17056284]
- Represa A, Jorquera I, Le Gal La Salle G, Ben-Ari Y. Epilepsy induced collateral sprouting of hippocampal mossy fibers: does it induce the development of ectopic synapses with granule cell dendrites? *Hippocampus*. 1993; 3(3):257–268. [PubMed: 8353609]
- Routtenberg A. Adult learning and remodeling of hippocampal mossy fibers: unheralded participant in circuitry for long-lasting spatial memory. *Hippocampus*. 2010; 20(1):44–45. [PubMed: 19554645]
- Ruediger S, Vittori C, Bednarek E, Genoud C, Strata P, Sacchetti B, Caroni P. Learning-related feedforward inhibitory connectivity growth required for memory precision. *Nature*. 2011; 473(7348):514–518. [PubMed: 21532590]
- Segal M, Olds J. Behavior of units in hippocampal circuit of the rat during learning. *J Neurophysiol*. 1972; 35(5):680–690. [PubMed: 5054511]
- Segal M, Andersen P. Dendritic spines shaped by synaptic activity. 2000; 10(5):582–586.
- Stettler DD, Yamahachi H, Li W, Denk W, Gilbert CD. Axons and synaptic boutons are highly dynamic in adult visual cortex. *Neuron*. 2006; 49(6):877–887. [PubMed: 16543135]
- Tashiro A, Dunaevsky A, Blazeski R, Mason CA, Yuste R. Bidirectional regulation of hippocampal mossy fiber filopodial motility by kainate receptors: a two-step model of synaptogenesis. *Neuron*. 2003; 38(5):773–784. [PubMed: 12797961]
- Teyler TJ, Rudy JW. The hippocampal indexing theory and episodic memory: updating the index. *Hippocampus*. 2007; 17(12):1158–1169. [PubMed: 17696170]
- Thompson LT, Moyer JR Jr, Disterhoft JF. Transient changes in excitability of rabbit CA3 neurons with a time course appropriate to support memory consolidation. *J Neurophysiol*. 1996; 73(3):1836–1849. [PubMed: 8890296]
- Toscano-Silva M, Gomes da Silva S, Scorza FA, Bonvent JJ, Cavalheiro EA, Arida RM. Hippocampal mossy fiber sprouting induced by forced and voluntary physical exercise. *Physiol Behav*. 2010; 101(2):302–308. [PubMed: 20515703]
- Treves A, Rolls ET. Computational constraints suggest the need for two distinct input systems to the hippocampal CA3 network. *Hippocampus*. 1992; 2:189–199. [PubMed: 1308182]
- Treves A, Rolls ET. Computational analysis of the role of the hippocampus in memory. *Hippocampus*. 1994; 4:374–391. [PubMed: 7842058]
- Vuksic M, Del Turco D, Bas Orth C, Burbach GJ, Feng G, Müller CM, Schwarzacher SW, Deller T. 3D-reconstruction and functional properties of GFP-positive and GFP-negative granule cells in the fascia dentata of the Thy1-GFP mouse. *Hippocampus*. 2008; 18(4):364–375. [PubMed: 18189310]
- Wenzel HJ, Cole TB, Born DE, Schwartzkroin PA, Palmiter RD. Ultrastructural localization of zinc transporter-3 (ZnT-3) to synaptic vesicle membranes within mossy fiber boutons in the hippocampus of mouse and monkey. *Proc Natl Acad Sci USA*. 1997; 94(23):12676–12681. PMID: PMC25081. [PubMed: 9356509]
- West RW, Greenough WT. Effect of environmental complexity on cortical synapses of rats: preliminary results. *Behav Biol*. 1972; 7(2):279–284. [PubMed: 5041867]

- Xu T, Yu X, Perlik AJ, Tobin WF, Zweig JA, Tennant K, Jones T, Zuo Y. Rapid formation and selective stabilization of synapses for enduring motor memories. *Nature*. 2009; 462(7275):915–919. [PubMed: 19946267]
- Yamahachi H, Marik SA, McManus JN, Denk W, Gilbert CD. Rapid axonal sprouting and pruning accompany functional reorganization in primary visual cortex. *Neuron*. 2009; 64(5):719–729. [PubMed: 20005827]
- Yang G, Pan F, Gan WB. Stably maintained dendritic spines are associated with lifelong memories. *Nature*. 2009; 462(7275):920–924. [PubMed: 19946265]
- Zhao C, Teng EM, Summers RG Jr, Ming GL, Gage FH. Distinct morphological stages of dentate granule neuron maturation in the adult mouse hippocampus. *J Neurosci*. 2006; 26(1):3–11. [PubMed: 16399667]

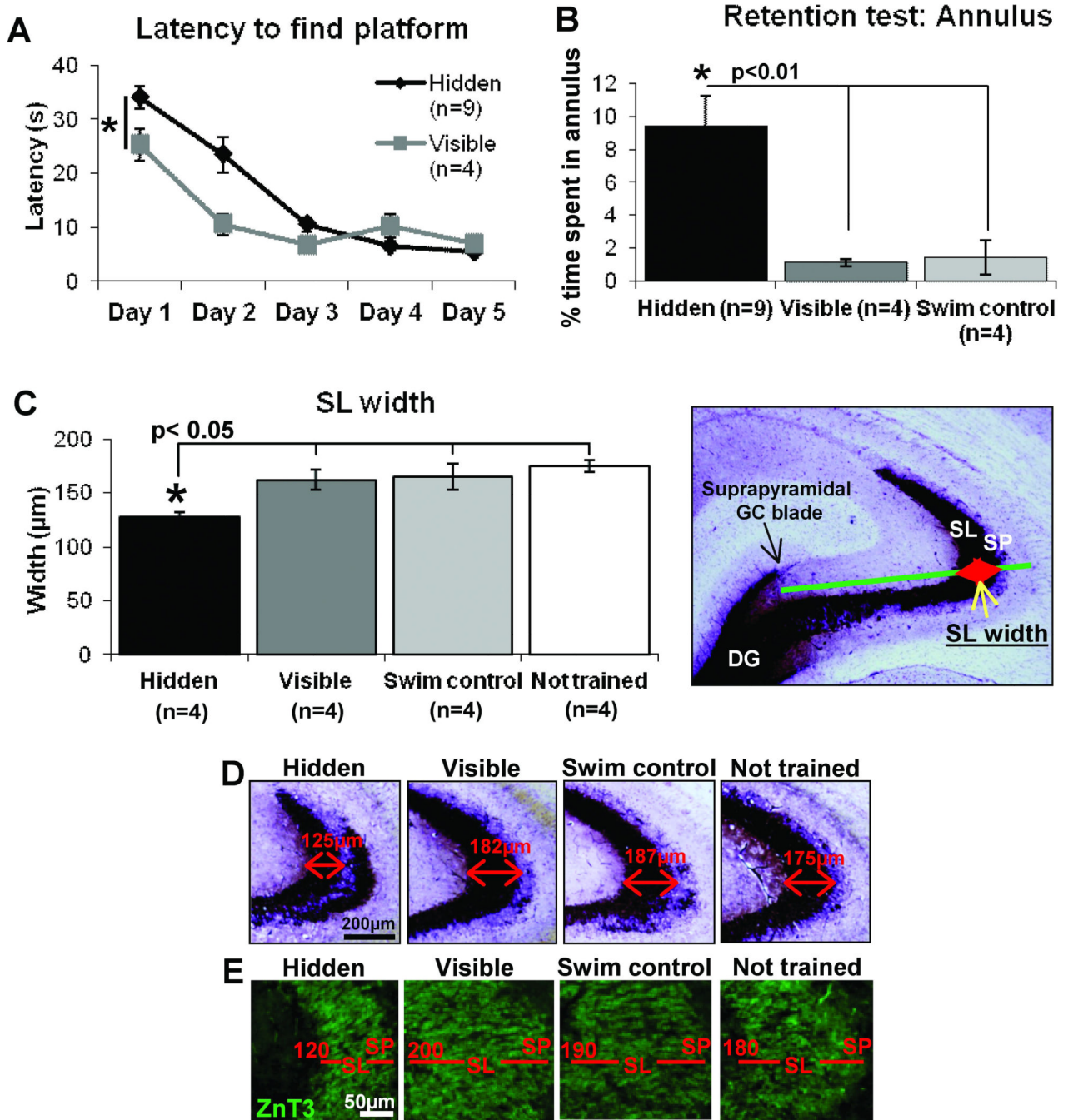


Figure 1. Learning-induced MF remodeling 7 days after the completion of water maze training. Adult Wistar rats trained for 5 d to find a hidden platform in a water maze using extramaze cues spend more time in the annulus area during the retention test, thereby demonstrating long-lasting memory. The analysis of the MF terminal field in SL compared to control groups reveals a ‘laminar thinning’ of that field. A) Latency to find the platform during training was initially faster in visible platform trained rats but by day 5 hidden and visible platform groups had comparable performance. B) During a retention test 7 days later, Hidden platform trained animals spent a significantly greater time in the annulus than control groups, demonstrating a better memory for the original platform location. C) The width of

the SL, established by Timm's staining, is significantly reduced (laminar thinning) in hidden platform trained animals compared to all other groups, which were not significantly different to each other. The procedure for measuring SL width in Timm's stained hippocampus from a control rat is superimposed onto the image to the right (D). Representative images of Timm's staining in the anterior hippocampus of each training group. SL width is indicated by the values above the red arrows. E) SL width was also identified by ZnT3 staining, examples from each training group illustrate the difference in laminar thinning, indicated by the value given in red. Scale bar= 200 μ m (D), 50 μ m (E), * p <0.05, ** p <0.01, repeated-measures ANOVA (A), One-way ANOVA (B and C).

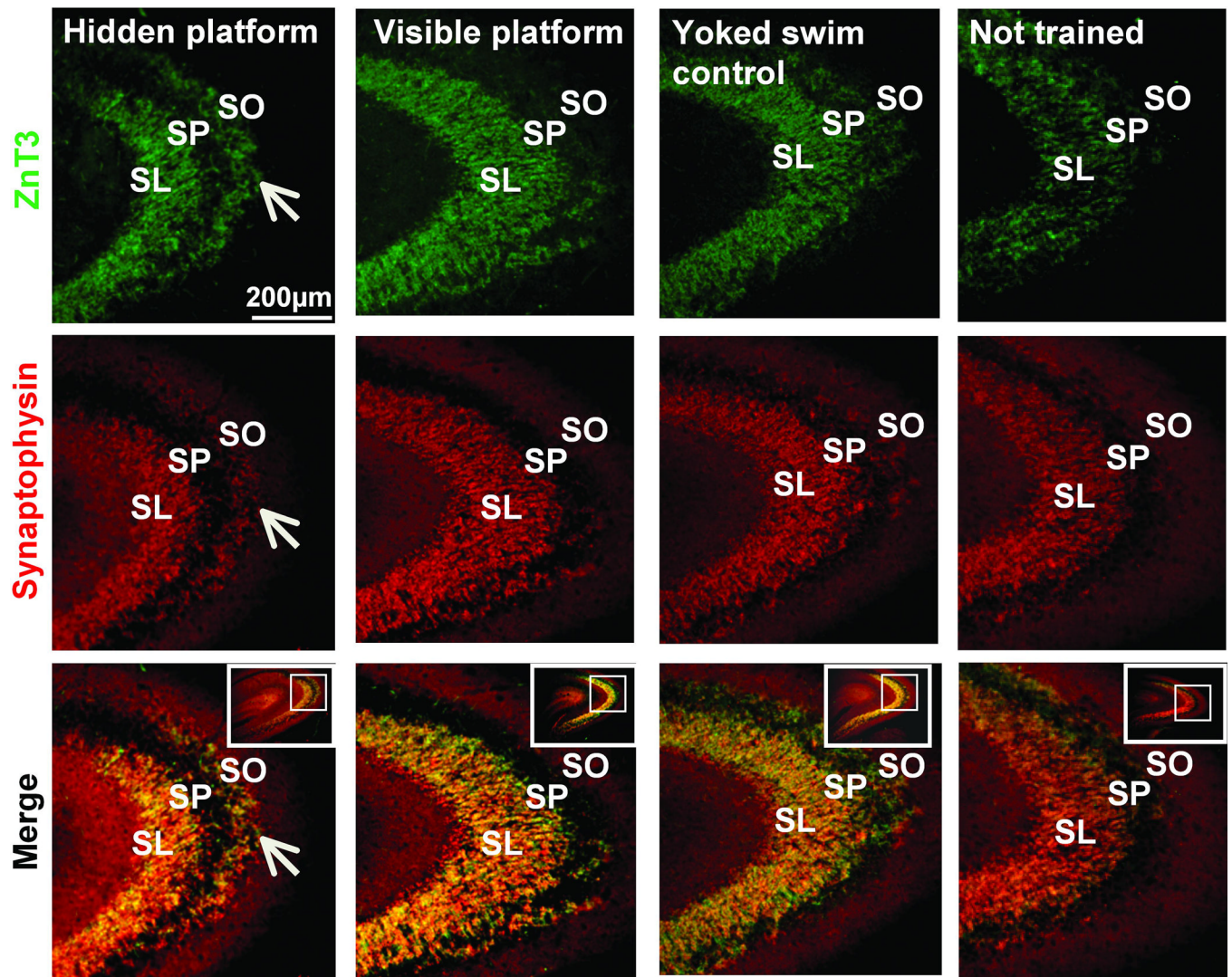


Figure 2. Learning induced ‘laminar thinning’ of SL and induction of a new layer of staining in SO identified both by ZnT3 and synaptophysin. Low power representative images doublestained for ZnT3 (*top*) and synaptophysin (*middle*) from each training group also illustrate the overlay (*bottom*) of these two markers. White arrows indicate prominent ZnT3 and synaptophysin staining in the SO in hidden platform trained rats; note the absence of ZnT3 staining in the SO of all other groups. Scale bar= 200µm.

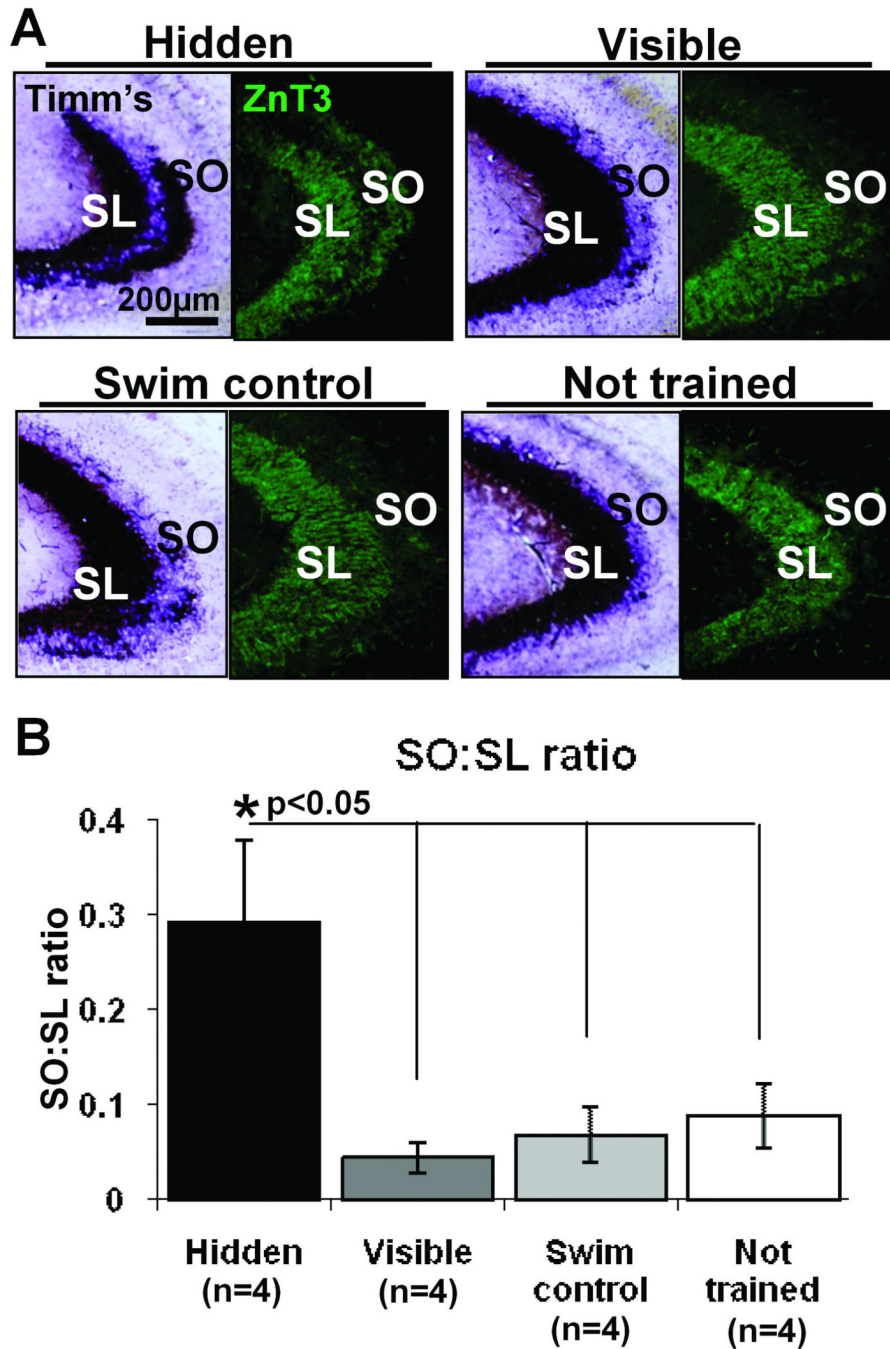


Figure 3. Hidden platform training induces translaminal growth giving rise to an induced expansion of MF terminal field into the SO. A) Comparison of Timm's staining (left) and ZnT3 immunofluorescent staining (right), two markers used to identify MF terminals, in the CA3 of each training group. Hidden platform trained animals have a visibly greater amount of staining for both histological markers in the SO compared to visible platform trained, yoked swim control and not trained rats. B) The growth into SO, as determined by the ratio of Timm's stained area in the SO compared to the SL, was significantly higher in hidden platform trained animals compared to all other training groups *p<0.05, One-way ANOVA., which were not significantly different from each other.

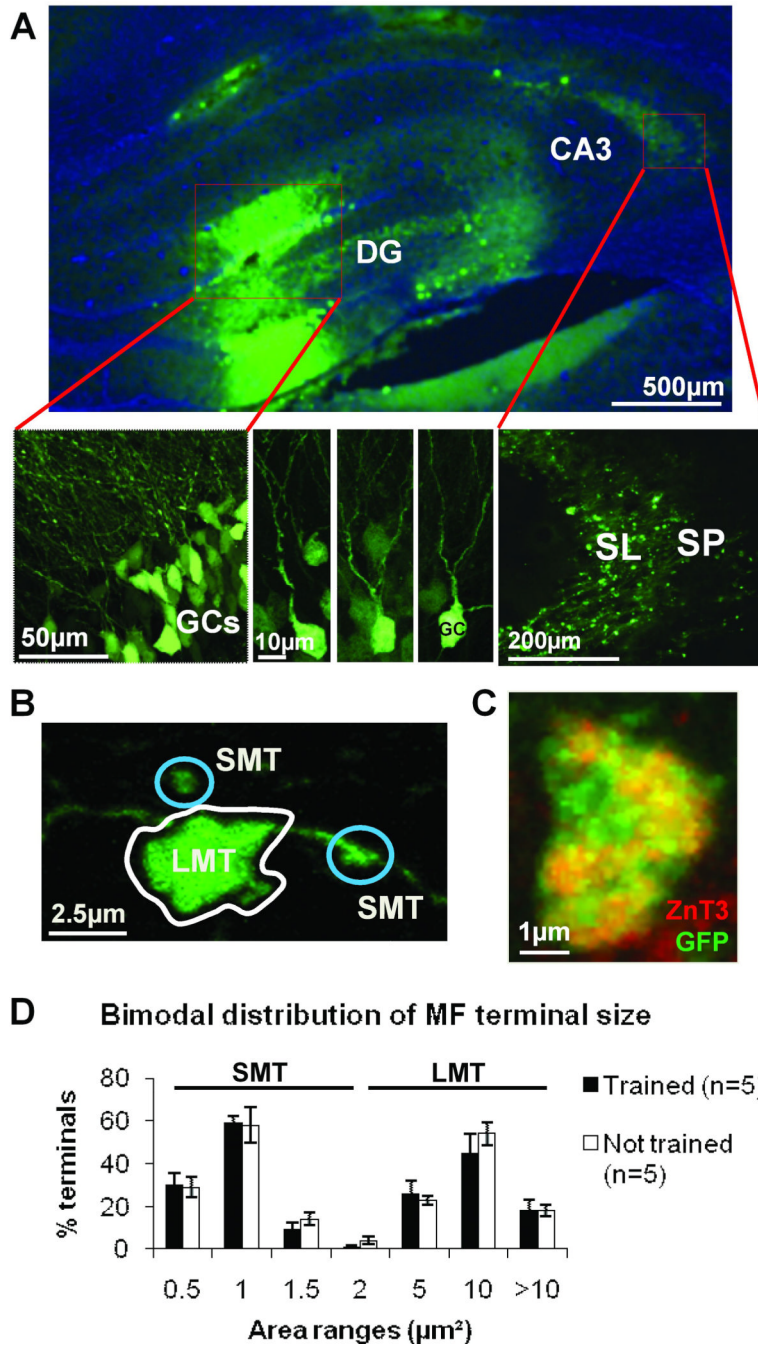


Figure 4. Bimodal distribution of terminal area illustrates the classification of small and large MF terminal subtypes (SMTs and LMTs, respectively). A) HSV-mediated GFP delivery to dentate gyrus: labeled GC layer (*lower left*); GC bodies and dendrites (*lower center*); MFs and their terminals in the SL (*lower right*). B) An example of a GFP labeled LMT and two SMT. C) HSV-GFP positive terminals can also be co-labeled with ZnT3 proving they are MF terminals. D) The various recorded areas of individual GFP-marked MF terminals does not adhere to a normal distribution (Shapiro-Wilks, $p < 0.05$) but instead follows a bimodal distribution, each mode has been designated SMT and LMT. Note that this pattern does not

change with training. Scale bars A) 500 μ m (upper), 50 μ m (lower left), 10 μ m (lower center), 200 μ m (lower right); B) 2.5 μ m; C) 1 μ m.

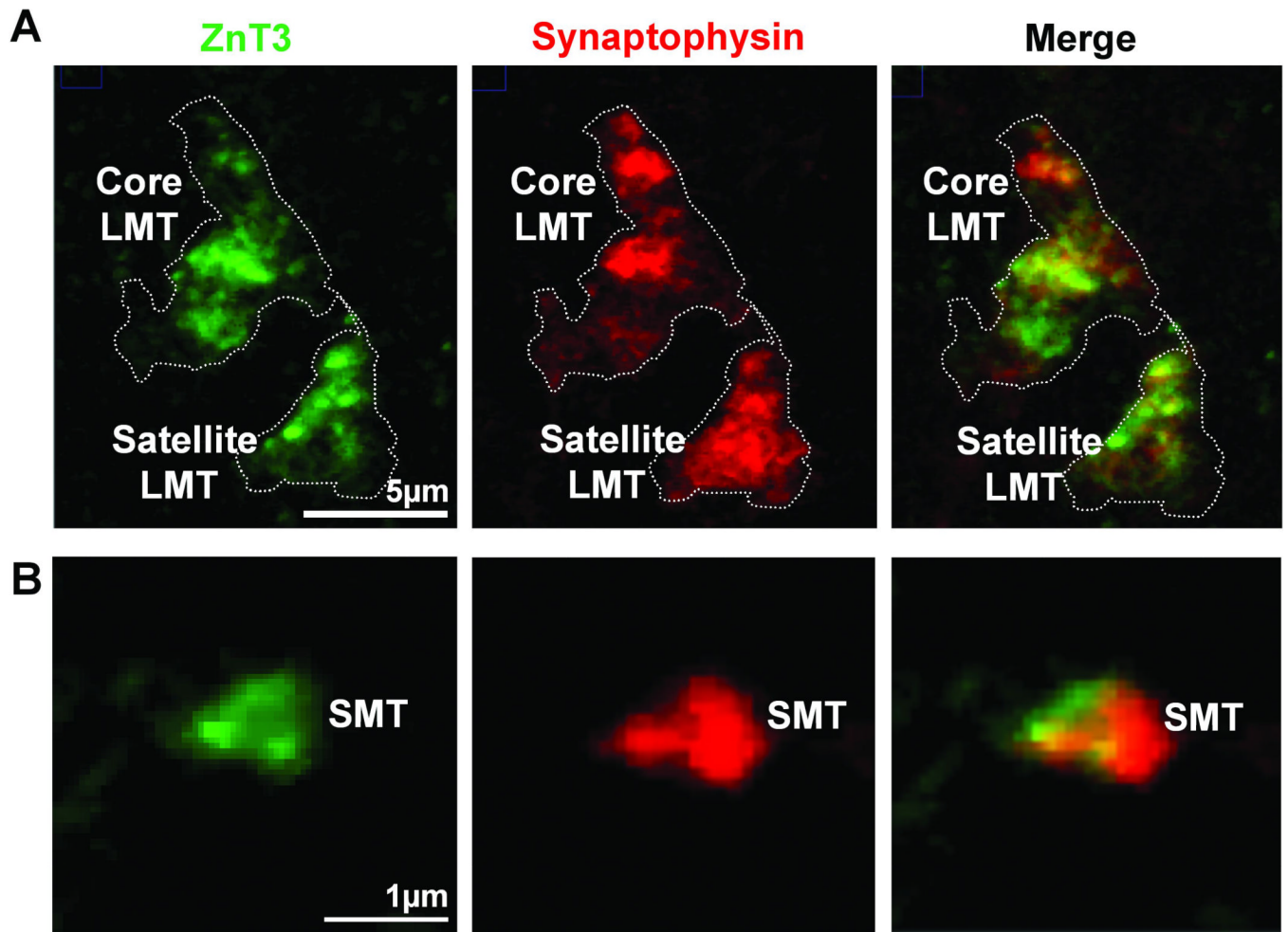


Figure 5. Identification of MF terminal subtypes by presynaptic markers, ZnT3 and synaptophysin. A) A maximum intensity projection of a confocal z-stack, depicting two LMT (one core LMT at the top and satellite LMT at the bottom) double-stained for ZnT3 and synaptophysin from the SO of a hidden platform trained rat. B) A single z-slice taken through an SMT labeled with ZnT3 and synaptophysin. Scale bars A) 5µm; B) 1µm.

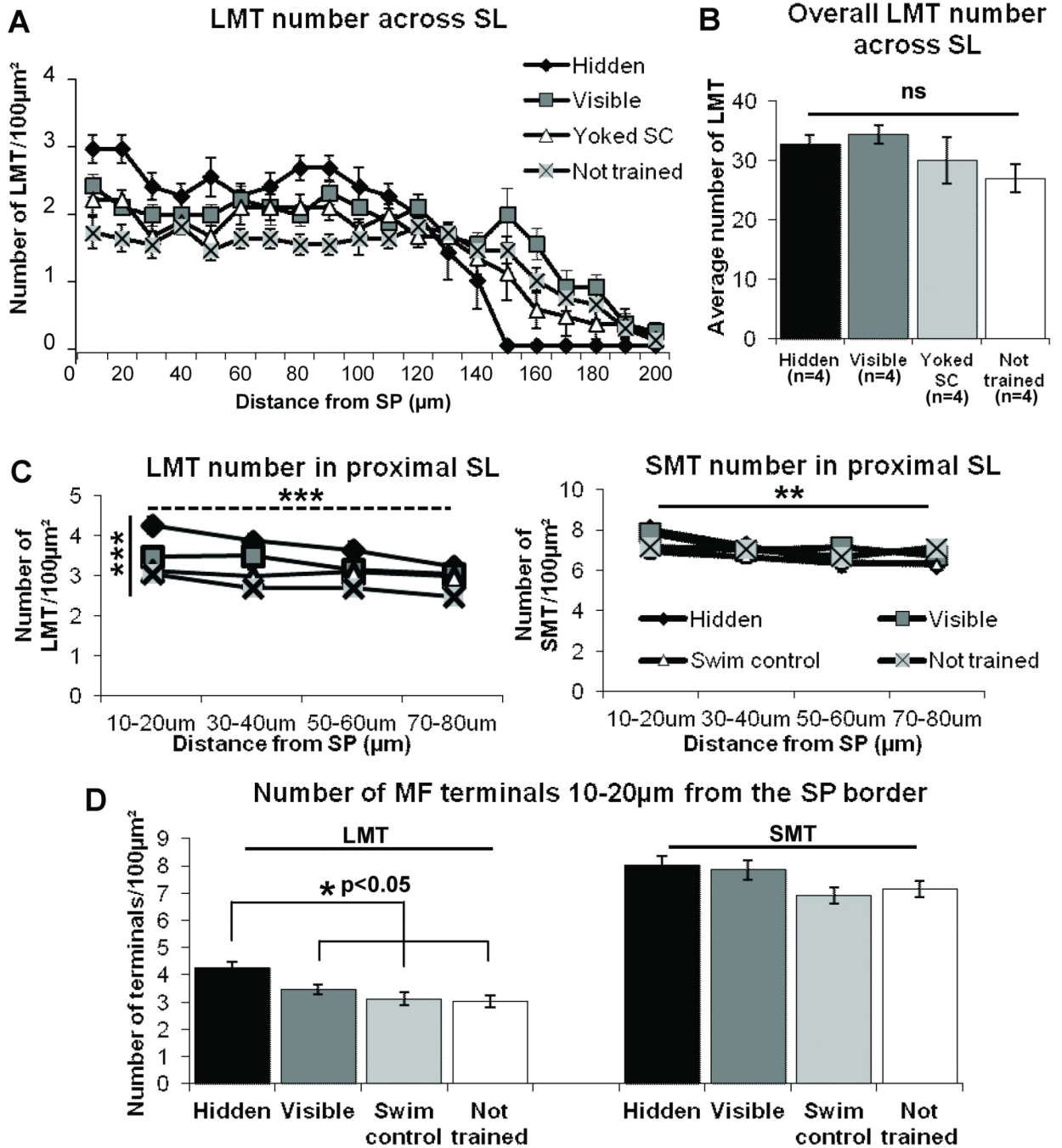


Figure 6. In the SL, spatial learning induces a redistribution of ZnT3 identified LMT such that there is a compression of this terminal type adjacent to the SP cell layer in Wistar rats. In what follows, significance values are shown on the graph. A) The number of LMTs significantly differs with distance from the SP border. B) Importantly, the total LMT number across the entire SL remains the same for all groups ($p=0.26$). C) The number of LMTs (*left*) significantly decreases with distance (dashed horizontal line) and significantly differs between groups (solid vertical line) in the most proximal region of SL to the SP border, while SMT number (*right*) significantly decreases with distance at the same rate for all groups (horizontal line) which are not significantly different from each other ($p=0.475$). D)

There is a significant increase in the number of LMT at the region closest to the SL/SP border (10–20 μ m) in the hidden platform trained group compared to all other training groups (*left*). There is no detectable change in SMT number among groups in the same region (*right*, $p=0.169$). Significance values shown on the graph are: * $p<0.05$, ** $p<0.01$, *** $p<0.001$, repeated-measures ANOVA (A and C), One-way ANOVA (B and D).

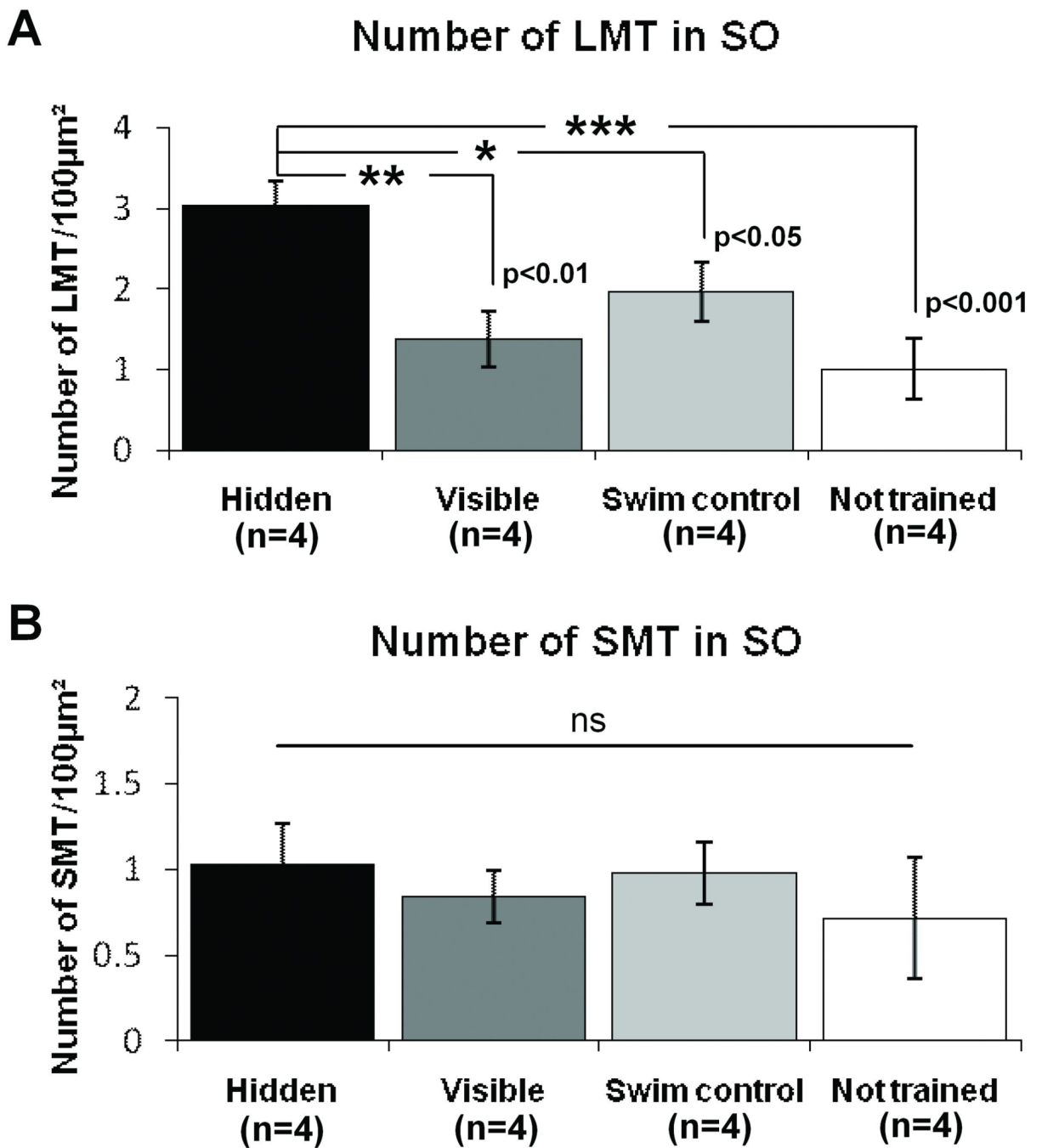


Figure 7.

In the SO, spatial learning induces an increase in LMT number. A) Hidden platform training in a water maze results in a significant increase in LMT number in the SO. There is no significant difference in LMT number among other groups. B) There is no significant difference in SMT number between training groups in the SO ($p=0.86$). * $p<0.05$, ** $p<0.01$, *** $p<0.001$, One-way ANOVA.

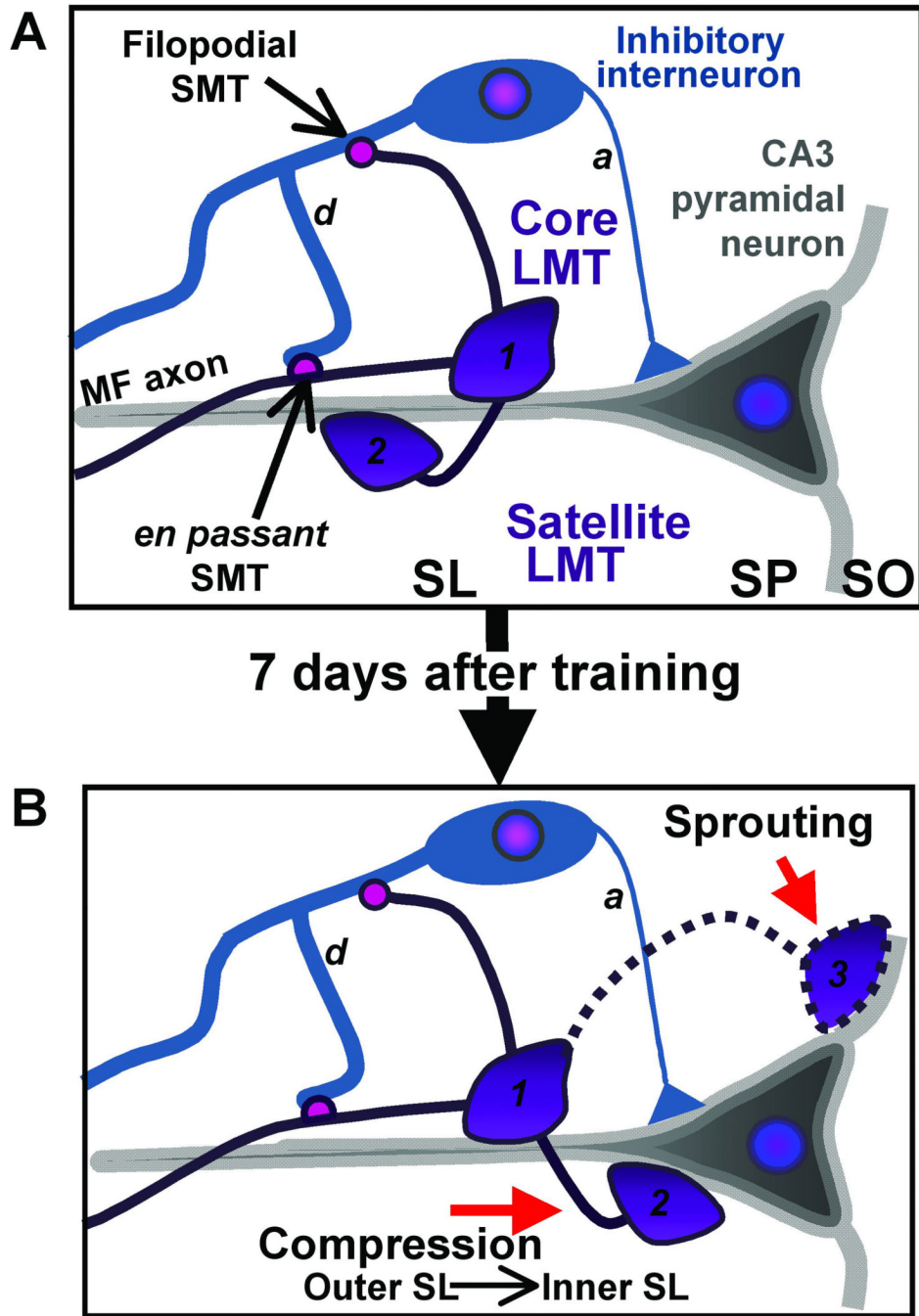


Figure 8. Cartoon illustrating the two MF terminal sub-types and their postsynaptic targets and the consequence of learning on remodeling. A) Large MF terminals (LMTs) are 2.5–10 μ m in diameter and are found in an *en passant* configuration along the MF axon or can exist at the end of a filopodial extension from a core LMT; this extension is designated a satellite LMT. The small MF terminals (SMTs) are 0.5–2 μ m in diameter and can also be found *en passant* along the MF axon or can form at the end of filopodial extensions arising from LMTs. The LMTs target the CA3 pyramidal cell apical dendrites in the SL while the SMTs target inhibitory interneurons. B) Two potential scenarios are considered here that may underlie learning-induced remodeling of hippocampal MFs. After learning, LMTs grow into the

stratum oriens (SO) and also rearrange in the SL. The former may arise as a result of *sprouting* of LMTs into SO from core terminals in SL, while the latter may occur as a consequence of *compression* of LMTs from the outer SL into the inner SL. *d*; dendrite; *a*; axon.